2020 IEEE/RSJ International Conference on Intelligent Robots and Systems (IROS)
October 25-29, 2020, Las Vegas, NV, USA (Virtual)

Dynamic Stability Control of Inverted-Pendulum-Type Robotic Wheelchair for Going Up and Down Stairs

Yuya Onozuka[1], Nobuyasu Tomokuni[2], Genki Murata[3], and Motoki Shino[1]

Abstract— **The wheelchair is the major means of transport for elderly and physically disabled people in their daily lives. However it cannot overcome architectural barriers such as curbs and stairs. In this study, we developed an inverted-pendulum-type robotic wheelchair for climbing stairs. The wheelchair has a seat slider and two rotary links between the front and rear wheels on each side. When climbing up stairs, the wheelchair rotates the rotary links while maintaining an inverted state of a movable body by controlling the position of the center of gravity using the seat slider. In previous research, we proposed the control method for climbing up stairs using the rotary links and seat slider, confirming a period of approximately 5 s to rotate the rotary links. In this paper, we propose a control method for going down stairs, and experimentally verify the control effectiveness and stability.**

I. INTRODUCTION

In recent years, the number of elderly and physically disabled people has increased, leading to a surge in the demand of electric-powered wheelchairs (EPWs). However, the difficulty to access areas with curbs and stairs using a standard EPW limits the scope of activities that can be completed, thus declining the quality of life of those who depend on EPWs. Various stair-climbing EPWs have been developed to access these areas without requiring external assistance. Most developed stair-climbing EPWs use wheels on flat terrain and special mechanisms on stairs or steps to maintain locomotion efficiency [1]. These mechanisms differ depending on the grounding method and are classified into three types: crawler, multipoint grounding, and two-point grounding.

The mechanism combining crawlers and wheels [2] [3] uses crawlers when going up and down stairs as well as wheels when traveling on flat ground. The crawler contact surface when climbing up stairs is the edge of the stairs. Consequently, on stairs with large gradient, the risk of slipping increases, and large motor torque is required. Therefore, crawlers are appropriate for stairs with small gradients. Zero Carrier [4], TBW-1 [5], and RT-Mover [6] with leg–wheel mechanism leverage multipoint grounding to maintain static stability by creating three or more ground contact points when climbing stairs. These mechanisms allow safe locomotion because static stability is constantly maintained. However, the mechanism is complicated, and the undercarriage is bulky. Although an active rotary-leg mechanism with compact undercarriage has been proposed [7], a one-way clutch is utilized to climb stairs, being impossible to go up and down stairs using the same mechanism. The iBOT [8] utilizes two-point grounding by using two right and left wheels and a rotary link that connects the front and rear wheels on each side. The iBOT climbs by alternating four- and two-point grounding, and provides a compact mechanism for going up and down stairs regardless of the stair slope and tread length. However, the statically unstable two-point grounding on stairs requires the user to hold the handrail to maintain balance while climbing up stairs without assistance of a caregiver [8]. Therefore, the iBOT is unsuitable for elderly people with limited lower- and upper-body function.

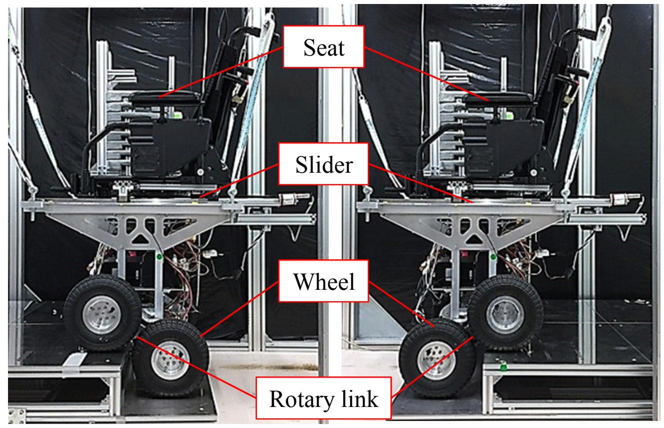

Fig. 1. Prototype of developed inverted-pendulum-type robotic wheelchair [12]. The left figure shows the wheelchair going up stairs and the right figure shows it going down stairs.

The EPW proposed by Shino et al. [9] uses two-point grounding similar to the iBOT, as shown in Fig. 1, and climbs up stairs using the control theory of an inverted pendulum. This EPW has a slider mechanism to control the center-of-gravity position. Unlike the iBOT, it autonomously adjusts balance, omitting the necessity of caregiver assistance or user training. In a previous study using this stair-climbing EPW, a controller was implemented to maintain the pitch angle at 0 rad without falling on the stairs [9] [10] [11] [12]. Consequently, stability was guaranteed by taking approximately 5 s to actuate the rotary links for climbing upstairs. However, the stability when going downstairs was not demonstrated. In this study, we developed a stair-climbing EPW with two-point grounding and center-of-gravity position control with

*This work was supported by JTEKT Co. Ltd.

[1]Yuya Onozuka and Motoki Shino are with the Department of Human and Engineered Environmental Studies, Graduate School of Frontier Sciences, The University of Tokyo, 5-1-5 Kashiwanoha, Kashiwa, Chiba, Japan onozuka.yuya@atl.k.u-tokyo.ac.jp motoki@k.u-tokyo.ac.jp

[2]Nobuyasu Tomokuni is with the Department of Robotics, Kindai University, 1 Takaya Umenobe, Higashi-Hiroshima, Hiroshima, Japan tomokuni@hiro.kindai.ac.jp

[3]Genki Murata is with JTEKT Corporation, 1-7 Kitajizozan, Noda-cho,Kariya, Aichi, Japan genki_murata@jtekt.co.jp

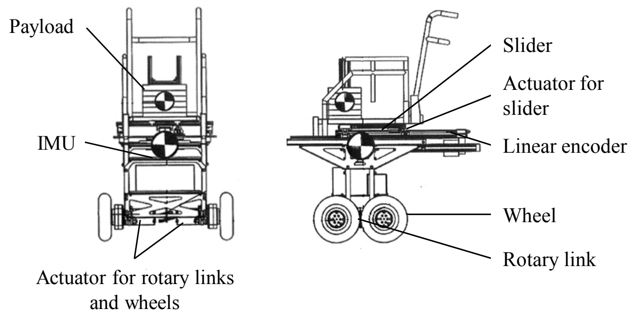

(a) Front view (b) Side view

Fig. 2. Mechanism of developed EPW (IMU, inertial measurement unit) [12]

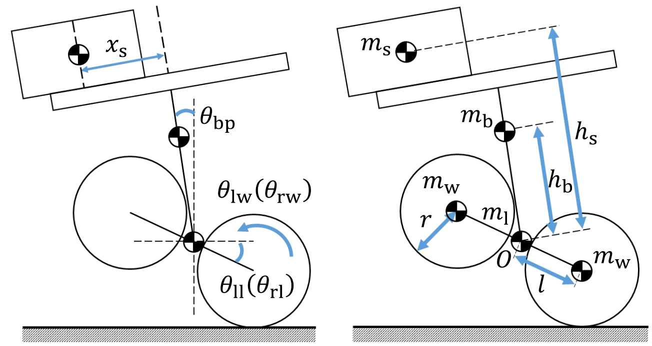

(a) State variables (b) Mass and length diagram

Fig. 4. Simplified model resembling inverted pendulum [12]

TABLE I
SPECIFICATIONS OF DEVELOPED EPW

Parameter	Value
Height	1245–1375 mm
Length	1055–1175 mm
Width	732 mm
Weight (without payload)	90 kg
Maximum thrust of slider actuator	895 N
Maximum motor torque of rotary link	150 Nm
Maximum motor torque of wheel drive	10 Nm

TABLE II
PARAMETERS OF DEVELOPED EPW

Parameter	Symbol	Value
Pitch angle of robot body	θ_{bp}	–
Rotation angle of left rotary link	θ_{ll}	–
Rotation angle of right rotary link	θ_{rl}	–
Rotation angle of left grounding wheel	θ_{lw}	–
Rotation angle of right grounding wheel	θ_{rw}	–
Slider displacement	x_{s}	–
Torque of left rotary link	τ_{ll}	–
Torque of right rotary link	τ_{rl}	–
Torque of left grounding wheel	τ_{lw}	–
Torque of right grounding wheel	τ_{rw}	–
Slider force	F_{s}	–
Wheel radius	r	0.125 m
Half-length of rotary link	l	0.13 m
Center of mass of body base	h_{b}	0.2528 m
Center of mass of seat	h_{s}	0.617 m
Mass of rotary link	m_{l}	7.4 kg
Mass of wheel	m_{w}	1.65 kg
Mass of body base	m_{b}	50.0 kg
Mass of slider (including payload)	m_{s}	98.5 kg
Total mass of wheelchair	M	169.9 kg
Inertia of wheel	J_{w}	0.00965 kgm^2
Inertia of rotary link	J_{l}	0.107 kgm^2

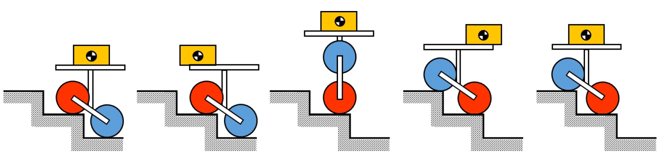

(a) (b) (c) (d) (e)

Fig. 3. Sequence for going up and down stairs [12]

a slider. In addition, we evaluated the stability while going down stairs and the effectiveness of the proposed control method.

II. DEVELOPED ROBOTIC WHEELCHAIR

A. Mechanical Design

Front and side views of the mechanism proposed by Shino et al. are depicted in Fig. 2, and its specifications are listed in Table I. The proposed mechanism comprises two rotary links between the front and rear wheels on each side, and a slider that moves the seat back and forth. The user is assumed to be fixed to the seat with a seat belt. As it has been experimentally confirmed that the behavior of this device has low effect on the user, a payload can substitute the real user [12]. The device has a slider actuator under the seat and rotary links and wheel-drive motors. Shino et al. evaluated stair climbing with these actuators, confirming that each actuator has the adequate frequency response [9]. In addition, this EPW has a sensor for each actuator, and an inertial measurement unit to acquire the pitch angle of the movable body. A public facility is assumed as the operation environment for this EPW, and the dimensions of stairs should satisfy the Japanese Building Standards [13].

B. Control System for Stair Climbing

Fig. 3 shows the sequence for the developed EPW to go up and down stairs. The EPW allows climbing upstairs by switching between two operation modes: center-of-gravity control (from Fig. 3(a) to (b) and from Fig. 3(d) to (e)) and rotary link control (from Fig. 3(b) to (d)). Similarly, the EPW allows going downstairs by adopting the inverse sequence from Fig. 3(e) to (a). The center-of-gravity control conforms a preparation phase for performing inverted pendulum control on the front wheels. The center of gravity of the movable body is placed above the front wheels by moving the slider when the front and rear wheels are in contact with the ground. During this phase, the slider moves to the target position, and proportional–differential control and gravity compensation are performed for the rotation of the rotary links and wheels to remain fixed. During rotary link control, the link is rotated for the wheels on stairs to be switched via inverted pendulum control on the two front wheels. During this phase, the target rotation for the rotary link is adjusted to the stair shape, and the target trajectories for the wheel rotation and the slider translation are calculated accordingly. Considering symmetrical control when going up and down stairs, a controller has been proposed based on the 2D rigid body model shown in Fig. 4 [12]. This controller combines feedforward control that provides actuator inputs to follow the target trajectory and feedback control that compensates for disturbances and modeling errors to improve trajectory tracking. The movement of the center of gravity caused by the slider during the corresponding phase can be easily controlled. The control methods during inverted state and mode transition are described below.

1) Control during Inverted State: We focus on the equation of motion (1) for maintaining the pitch angle at 0 rad when setting the target trajectory for each state variable:

$$0 = \frac{d}{dt}\left(\frac{\partial L}{\partial \dot{\theta}_{\mathrm{bp}}}\right) - \frac{\partial L}{\partial \theta_{\mathrm{bp}}}, \tag{1}$$

where t represents time and L is the Lagrangian function.

When (1) is expanded using $\theta_{\mathrm{bp}} = \dot{\theta}_{\mathrm{bp}} = \ddot{\theta}_{\mathrm{bp}} = 0$, $\theta_{rl} = \theta_{\mathrm{ll}} = \theta_{\mathrm{l}}$, and $\theta_{\mathrm{rw}} = \theta_{\mathrm{lw}} = \theta_{\mathrm{w}}$, it can be expressed as (2), where the total weight of the wheelchair, $(4m_{\mathrm{w}}+2m_{\mathrm{l}}+m_{\mathrm{b}}+m_{\mathrm{s}})$, is denoted as M.

$$\begin{aligned}
0 = &-m_{\mathrm{s}} g x_{\mathrm{s}} + Mgl\cos\theta_{\mathrm{l}} \\
&+ (4J_{\mathrm{w}} + (Mr + m_{\mathrm{s}}h_{\mathrm{s}} + m_{\mathrm{b}}h_{\mathrm{b}} + Ml\sin\theta_{\mathrm{l}})r)(\ddot{\theta}_{\mathrm{w}} + \ddot{\theta}_{\mathrm{l}}) \\
&+ m_{\mathrm{s}}(r + h_{\mathrm{s}} + l\sin\theta_{\mathrm{l}})\ddot{x}_{\mathrm{s}} \\
&+ (4J_{\mathrm{l}} + (M + 4m_{\mathrm{w}})l^2)\ddot{\theta}_{\mathrm{l}} \\
&+ (Mr + m_{\mathrm{s}}h_{\mathrm{s}} + m_{\mathrm{b}}h_{\mathrm{b}})l(\ddot{\theta}_{\mathrm{l}}\sin\theta_{\mathrm{l}} + \dot{\theta}_{\mathrm{l}}^2\cos\theta_{\mathrm{l}}) \\
&- m_{\mathrm{s}}x_{\mathrm{s}}l(\ddot{\theta}_{\mathrm{l}}\cos\theta_{\mathrm{l}} - \dot{\theta}_{\mathrm{l}}^2\sin\theta_{\mathrm{l}})
\end{aligned} \tag{2}$$

Each term in (2) represents a moment acting on the pitch angle, and this is the conditional equation for maintaining $\theta_{\mathrm{bp}} = 0$. Although the proposed EPW has six degrees of freedom ($\theta_{\mathrm{bp}}, \theta_{\mathrm{ll}}, \theta_{\mathrm{rl}}, \theta_{\mathrm{lw}}, \theta_{\mathrm{rw}}$ and x_{s}), no actuator driving the pitch angle is available, establishing an underactuated robot controlled by five actuators. Therefore, it is not possible to plan target trajectories for the six variables independently. In fact, if a target trajectory with five degrees of freedom is determined, the trajectory for the remaining degree of freedom is automatically determined [14]. Hence, once the desired trajectories of two of three variables (e.g., x_{s}, θ_{l}, and θ_{w}) are determined, the trajectory for the remaining variable is uniquely determined to satisfy (2) under $\theta_{\mathrm{bp}} = \dot{\theta}_{\mathrm{bp}} = \ddot{\theta}_{\mathrm{bp}} = 0$, $\theta_{\mathrm{rl}} = \theta_{\mathrm{ll}} = \theta_{\mathrm{l}}$, and $\theta_{\mathrm{rw}} = \theta_{\mathrm{lw}} = \theta_{\mathrm{w}}$.

In previous studies [11] [12], the target trajectory for the rotary link was first set for each section shown in Fig. 5, and then the target trajectory for the slider was set according to (3) for the moment around the grounding wheel in Fig. 4 to be geometrically zero. With this slider trajectory, the static equilibrium of the pitch angle can be maintained. However, moment M_{d} due to inertial force and the reaction of driving force acting on the pitch angle cannot be compensated.

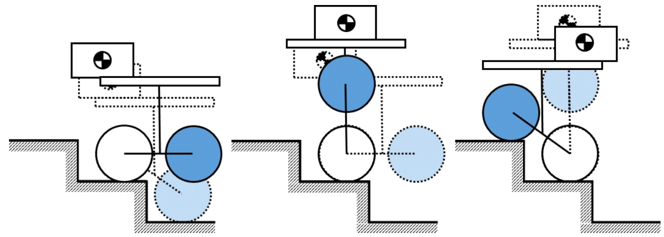

Fig. 5. Three sections during rotary link control. The sequence from sections 1 to 3 is utilized when climbing upstairs and that from section 3 to 1 is utilized when going downstairs. [12]

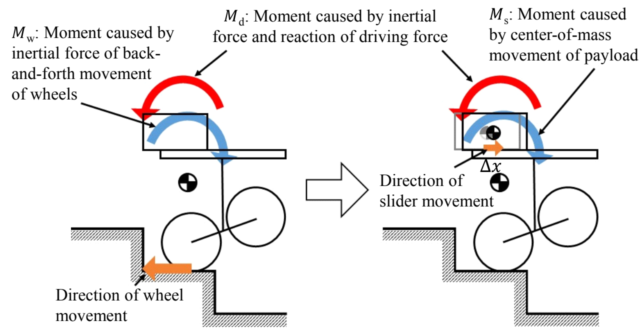

Fig. 6. Control considering dynamic equilibrium of pitch angle [12]

$$x_{\mathrm{sref}} = \frac{1}{2}\frac{Ml}{m_{\mathrm{s}}}(\cos(\theta_{\mathrm{rl}}) + \cos(\theta_{\mathrm{ll}})) \tag{3}$$

Onozuka et al. [12] clarified that the developed EPW generates moment M_{w} by the inertial force of the back-and-forth acceleration of the grounding wheels, as shown in the second term of (2) during stair climbing, to compensate for moment M_{d}. This grounding wheel acceleration increases with the rotary link angular velocity, leading to fall of the EPW in the worst case. Therefore, we propose a control method to generate moment M_{s} equivalent to M_{w} by displacing the center of gravity via slider motion to suppress the grounding wheel movement, as shown in Fig. 6.

Onozuka et al. also showed that grounding wheel acceleration $\hat{\ddot{x}}_{\mathrm{w}}$ can be estimated from rotary link angular velocity $\dot{\theta}_{\mathrm{l}}$ and designed a controller to generate moment M_s due to slider movement Δx derived from $\hat{\ddot{x}}_{\mathrm{w}}$ [12]. At this time, Δx is expressed as (4) from the relationship between the moment given by the second term in (2) and the moment due to the EPW center-of-gravity displacement. By using Δx, the slider target trajectory considering dynamic equilibrium of the pitch angle can be expressed by (5).

$$\Delta x = -\frac{4J_{\mathrm{w}} + (Mr + m_{\mathrm{s}}h_{\mathrm{s}} + m_{\mathrm{b}}h_{\mathrm{b}} + Ml\sin\theta_{\mathrm{l}})r}{m_{\mathrm{s}}gr}\hat{\ddot{x}}_{\mathrm{w}} \tag{4}$$

$$x_{\mathrm{srefdyn}} = \frac{1}{2}\frac{Ml}{m_{\mathrm{s}}}(\cos(\theta_{\mathrm{rl}}) + \cos(\theta_{\mathrm{ll}})) + \Delta x \tag{5}$$

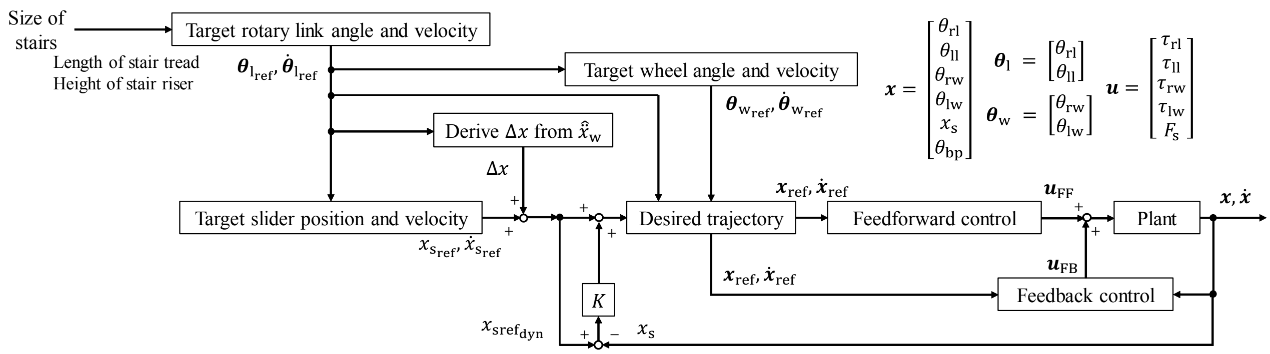

Fig. 7. Control block diagram of EPW for going up and down stairs [12]

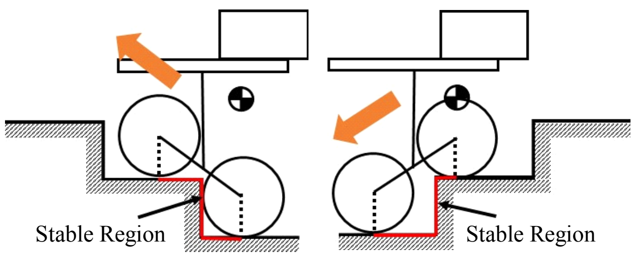

(a) Stable region when climbing upstairs (b) Stable region when going downstairs

Fig. 8. Stable region during four-wheel grounding of developed EPW

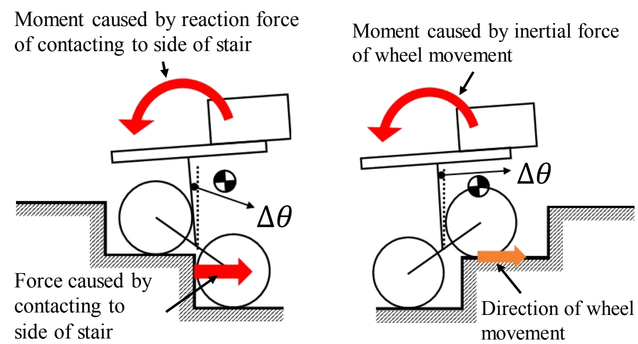

(a) Stabilization when climbing upstairs (b) Stabilization when going downstairs

Fig. 9. Stabilization strategy during mode transition

However, as mentioned in [12], when $\hat{\ddot{x}}_{\mathrm{w}} < 0$, $\Delta x = 0$. This control of slider displacement by Δx was applied from sections 2 to 3 in Fig. 5 for climbing upstairs, and from sections 3 to 2 for going downstairs. Fig. 7 shows the control block diagram of the proposed controller.

2) Mode Transition: Shifting from rotary link control to center-of-gravity control corresponds to shifting from the two-wheel inverted state to the four-wheel grounding state. During this transition, the target slider position should ensure that the center-of-gravity of the wheelchair at the end of rotary link control is on the contact point of the grounding wheels. However, the feedback gain during inverted state is the largest for the pitch angle, and other state variables have some deviated values to maintain the pitch angle 0 rad. For instance, the slider position has the deviated value σ of approximately ± 0.005 m from the target value. When this deviated value is in the opposite direction with respect to the target value, a backward moment is generated at mode transition, and the developed EPW falls. The following conditions must be satisfied to prevent tipping over due to the deviated value of slider position σ.

1) The dynamic EPW center-of-gravity is within the stable region at the end of two-wheel inverted control.
2) The static EPW center-of-gravity is within the stable region after landing.

The stable regions for going up and down stairs are shown as red lines in Fig. 8.

As shown in Fig. 9, condition 1 is satisfied with a forward moment generated by contacting the grounding wheel to the side of the stairs when climbing upstairs and driving the grounding wheels backward when going downstairs. To satisfy condition 2, we set the target rotary link angle such that the pitch angle tilts $\Delta\theta$ after landing and the EPW center-of-gravity is kept within the stable region. Moment variation ΔM_θ caused by tilting the pitch angle by $\Delta\theta$ is expressed as (6) and it controls the position of the EPW center-of-gravity. In addition, moment variation ΔM_σ due to the deviated value of slider position σ is expressed as (7). The pitch angle should be tilted by $\Delta\theta$ satisfying $\Delta M_\theta + \Delta M_\sigma > 0$, and the $\Delta\theta$ varies with σ as shown in Fig. 10.

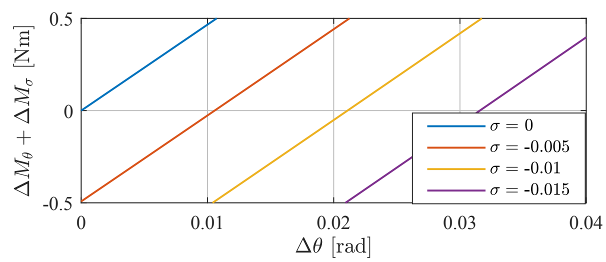

Fig. 10. Relationship between pitch angle $\Delta\theta$ after landing and moment variation ΔM_θ generated by pitch angle and ΔM_σ generated by slider position deviation σ

$$\Delta M_\theta = (m_{\mathrm{s}}h_{\mathrm{s}} + m_{\mathrm{b}}h_{\mathrm{b}})g\sin(\Delta\theta) - m_{\mathrm{s}}x_{\mathrm{s}}g(1-\cos(\Delta\theta)) \tag{6}$$

$$\Delta M_\sigma = m_{\mathrm{s}}g\sigma \tag{7}$$

Considering $x_{\rm s} = -0.2$ m and $\sigma = -0.005$ m for going downstairs, $\Delta M_\theta + \Delta M_\sigma > 0$ is satisfied at $\Delta\theta > 0.011$. Therefore, the target rotary link angle is set to a value such that the pitch angle $\Delta\theta$ after landing is larger than 0.11 rad to satisfy the condition 2.

III. EXPERIMENTS AND RESULTS

A. Experimental Setup

To verify the effectiveness and stability of the proposed controller for going downstairs, we conducted experiments considering a payload of 80 kg substituting a user and time T for the rotary link control of 6 s. Adhering to the Japanese Building Standards, the height of the stairs was 0.14 m and the length of the stairs was 1.0 m. In addition, the experiment was conducted for $T = 15$ s as condition under which the effect of both inertial force and reaction of the driving force was small. The developed EPW had no functions to sense the surrounding environment, and the stair-height information measured for control was given.

B. Experimental Results

We analyzed the results during rotary link control and mode transition. Fig. 11 shows the amount of grounding wheel movement during rotary link control over 15 s. Under this condition, the effect of the inertial force and reaction of the driving force is small, and hence Δx obtained from the estimated value of the grounding wheel acceleration $\hat{\ddot{x}}_{\rm w}$ is always 0 m. Hence, the target position of the slider statically maintains equilibrium of the pitch angle, and the grounding wheel movement is within the allowed range, which is calculated as the range for which the grounding wheels do not collide with the side of the stairs or slip off the edge of the stairs during grounding for step length of 0.26 m (i.e., the shortest length in public facilities).

Figs. 12 and 13 show the results for rotary link control during 6 s. Fig. 12 shows that the grounding wheels moved approximately 0.4 m before adding the control considering dynamic equilibrium of the pitch angle. However, by updating the target position of the slider by Δx and generating $M_{\rm s}$ as shown in Fig. 13, the amount of grounding wheel movement remained within the allowed range. The white wheel markers from 0 to 6 s in Fig. 14 show that the grounding wheels (front wheels) hardly moved. Fig. 15 shows the maximum variation of pitch angle and grounding wheel displacement in the inverted state under rotary link control over periods of 6 and 15 s. The pitch angle was kept around 0 rad and the maximum grounding wheel displacement was within the allowed range, demonstrating that the developed EPW can go downstairs at different speeds.

Fig. 16 shows the pitch angle during mode transition, with the period up to 6 s representing the rotary link control and the landing instant occurring at 7 s. At mode transition, the EPW landed without falling over by driving the grounding wheels backward. In addition, the pitch angle after landing was approximately 0.03 rad, satisfying $\Delta\theta > 0.011$ as shown in Fig. 16, and the static stability after landing was maintained by keeping the EPW center of gravity within the stable region.

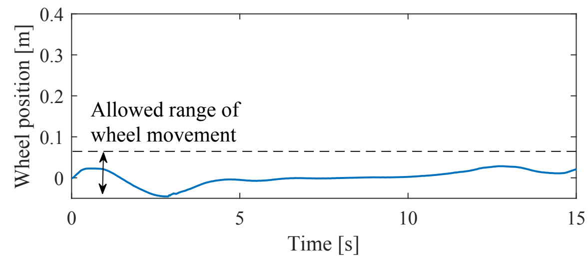

Fig. 11. Wheel position when going downstairs for T = 15 s

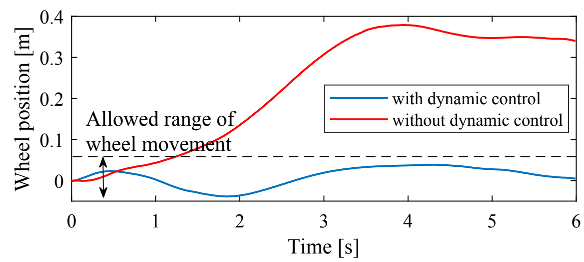

Fig. 12. Wheel position when going downstairs for T = 6 s

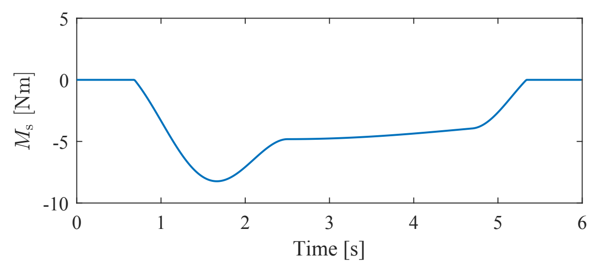

Fig. 13. Moment generated by center-of-mass movement of payload ($M_{\rm s}$)

C. Limitations

There were several limitations of the present study. Especially, the stair-height and the mass of a user were given as information for the control design. Therefore, further studies are necessary to clarify the effects of the measurement error and the modeling error on dynamic stability. Moreover, the dynamic stability under disturbances such as user movement has not been studied, and it is necessary to improve the functional safety when a user operates the EPW.

IV. CONCLUSIONS

We propose a control strategy to improve the dynamic stability for going up and down stairs using an underactuated stair-climbing EPW that utilizes two-point grounding and center-of-gravity position control by a slider.

- For control in inverted state, we designed a controller to determine the target trajectory of the slider considering dynamic equilibrium of the pitch angle.
- When shifting from the two-wheel inverted state to the four-wheel grounded state, we designed a controller to keep the center of gravity within the stable region, where the front and rear wheels touch the ground

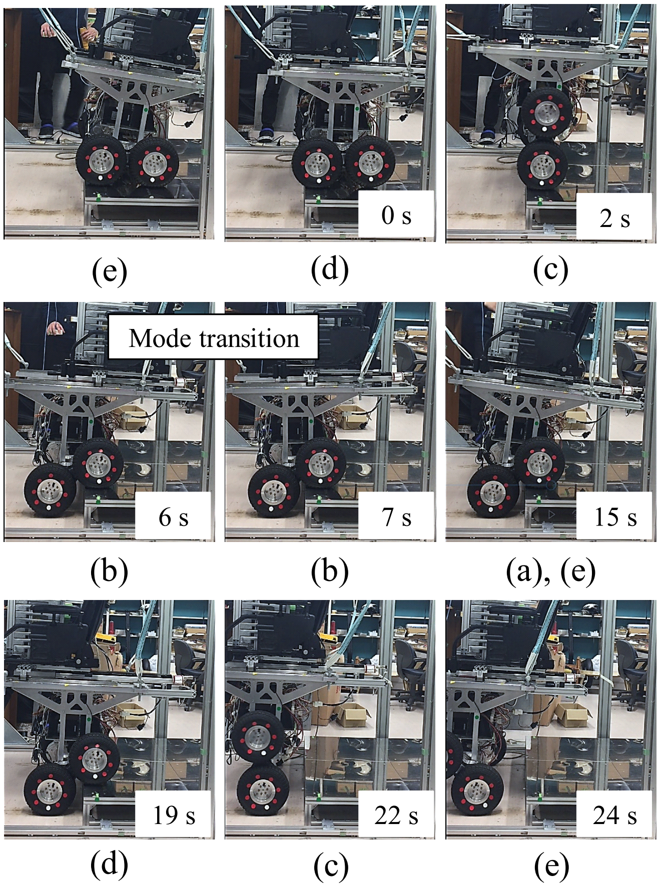

Fig. 14. Photographs of experiment sequence using proposed control to go downstairs. The sequence letters from (a) to (e) correspond to the stages shown in Fig. 3.

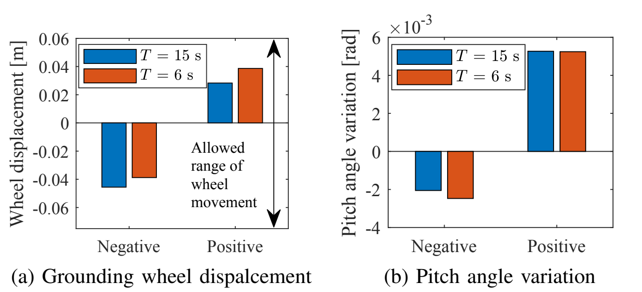

Fig. 15. Maximum grounding wheel displacement and pitch angle variation when going downstairs

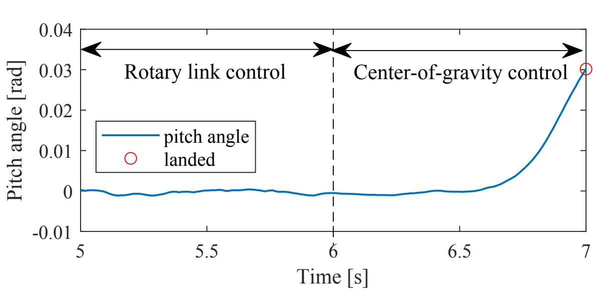

Fig. 16. Pitch angle during mode transition

considering the EPW center-of-gravity position and behavior.

- By applying the abovementioned controllers to the developed EPW, we demonstrated that the grounding wheels hardly move and stably go down stairs for rotary link control lasting 15 or 6 s and step height of 0.14 m.

Therefore, we demonstrated that the developed EPW can go up and down stairs at different speeds under the condition that a payload of 80 kg was substituted for a user. In future work, we will improve the functional safety when a user operates the EPW and propose corresponding safety measures. In addition, we have to equip the EPW with functions to sense the surrounding environment and verify the stability when measurement errors occur.

References

[1] W. Tao, J. Xu, and T. Liu, "Electric-powered wheelchair with stair-climbing ability," *Int. J. Adv. Robot. Syst.*, vol. 14, no. 4, pp. 1–13, July 2017.

[2] W. Tao, Y. Jia, T. Liu, J. Yi, H. Wang, and Y. Inoue, "A novel wheel-track hybrid electric powered wheelchair for stairs climbing," *J. Adv. Mech. Des. Syst. Manuf.*, vol. 10, no. 4, pp. 1–21, 2016.

[3] J. Podobnik, J. Rejc, S. Slajpah, M. Munih, and M. Mihelj, "All-terrain wheelchair: Increasing personal mobility with a powered wheel-track hybrid wheelchair," *IEEE Robot. Autom. Mag.*, vol. 24, no. 4, pp. 26–36, Nov. 2017.

[4] D. Davies and S. Hirose, "Continuous high-speed climbing control and leg mechanism for an eight-legged stair-climbing vehicle," in *2009 IEEE/ASME International Conference on Advanced Intelligent Mechatronics (AIM)*, pp. 1606–1612, July 2009.

[5] Y. Sugahara, N. Yonezawa, and K. Kosuge, "A novel stair-climbing wheelchair with transformable wheeled four-bar linkages," in *2010 IEEE/RSJ International Conference on Intelligent Robots and Systems (IROS)*, pp. 3333–3339, Oct. 2010.

[6] S. Nakajima, "Evaluation of the mobility performance of a personal mobility vehicle for steps," *IEEE Access*, vol. 5, pp. 9748–9756, May 2017.

[7] K. Sasaki and K. Suzuki, "Active rotary-legs mechanism for stair-climbing mobility vehicle," *IEEE Robot. Autom. Lett.*, vol. 3, no. 3, pp. 2237–2244, Mar. 2018.

[8] H. Uustal and J. L. Minkel, "Study of the independence IBOT 3000 mobility system: An innovative power mobility device, during use in community environments," *Arch. Phys. Med. Rehabil.*, vol. 85, no. 12, pp. 2002–2010, Dec. 2004.

[9] M. Shino, N. Tomokuni, G. Murata, and M. Segawa, "Wheeled inverted pendulum type robotic wheelchair with integrated control of seat slider and rotary link between wheels for climbing stairs," in *2014 IEEE International Workshop on Advanced Robotics and its Social Impacts (ARSO)*, pp. 121–126, Sept. 2014.

[10] N. Ding, M. Shino, N. Tomokuni, and G. Murata, "Fall avoidance control of wheeled inverted pendulum type robotic wheelchair while climbing stairs," *Int. J. Biomed. Biol. Eng.*, vol. 11, no. 4, pp. 168–175, Mar. 2017.

[11] R. Kawahata, M. Shino, S. Ota, N. Tomokuni, and G. Murata, "Motion control of pendulum type robotic wheelchair considering mutual interference behavior between wheel and rotary links in climbing stairs," *Proc. JSME Annu. Conf. Robot. Mechatronics*, vol. 2018, no. 1P2-G06, pp. 1–4, 2018 [in Japanese].

[12] Y. Onozuka, N. Tomokuni, G. Murata, and M. Shino, "Attitude control of an inverted-pendulum-type robotic wheelchair to climb stairs considering dynamic equilibrium," *Robomech J.*, vol. 7, no. 23, pp. 1–13, May 2020.

[13] Enforcement Ordinance of Construction Standard Law, Articles 23–27, 1950.

[14] H. Arai and S. Tachi, "Dynamic control of a manipulator with passive joints in an operational coordinate space," in *Proceedings 1991 IEEE International Conference on Robotics and Automation (ICRA)*, vol. 2, pp. 1188–1194, Jan. 1991.